

Dynamic behaviour of a linear superconducting levitation transport system using YBCO bulk material

Lars Kühn

IFW Dresden, Department 21, Helmholtzstr. 20, 01069 Dresden, Germany

Matthias Müller, Rainer Schubert, Cristoph Beyer, Oliver de Haas and Ludwig Schultz

IFW Dresden, Department 21, Helmholtzstr. 20, 01069 Dresden, Germany

ABSTRACT: The technical progress to manufacture high temperature superconducting bulk material (HTS) provides various possible applications. This involves non-contact linear transport systems and frictionless rotating bearings using the pinning effect in Typ-II superconductors. During the last five years a group of industrial and research partners have developed an innovative magnetic levitation system (SupraTrans) with a permanent magnetic rail and YBCO superconducting bulks in the vehicle. To optimize the levitation and guidance system further investigations in the static and dynamic behaviour have been accomplished and are reported. Comparisons between the statics, the dynamics and the simulation show a very well agreement in all comparable parameters

1 INTRODUCTION

Linear superconducting bearings are one possible application of high- T_C superconductors; utilize non-contact and passive-stable levitation by the pinning effect. An arrangement of permanent magnets (pm) works as the excitation-part of a superconducting bearing and determine the bearing stability depending on the excitation-design. After the superconducting bulk is cooled down below the critical temperature in the magnetic field of the permanent magnet, the interaction between the magnetic field and the vortex lines within the superconductor enable levitation.

In the mechanical design of superconducting magnetic bearing, such as linear transportation system, it is important to evaluate the static and dynamic characteristics based on the interaction between the permanent magnet and the superconducting bulk. This research experimentally and analytically investigates statics, dynamics and the stability of HTS-levitation systems. Research teams all over the world work on superconducting magnetic bearings (SMB), some of them reported static properties (de Haas et al. 2004, Beyer et al. 2004, Hull et al. 1999, Weinberger et al. 1990) and other reported dynamic and mechanical stability (Futamura et al. 1998, Sugiura et al. 1997) of superconducting levitation systems.

In this paper a preliminary assessment of the functionality of substitution of the linear superconducting magnetic bearings by a harmonic oscillator

is presented. Two apparatuses for measurements of static and dynamic characteristics of the levitation system are described and the measurement results are reported. The paper shows an interesting way to design a SMB for a special technical application and their requirements in four steps.

2 EXPERIMENTAL PROCEDURE

2.1 Force measurements

The schematic of the experimental arrangement is shown in fig. 1. The excitation part consists of two Nd-Fe-B permanent magnets with polarization in opposite direction and three Fe-flux-collectors mounted on a computer-controlled xy-stage.

The levitation part is made of a cubical melt-textured YBCO bulk (30 mm in diameter and 15 mm in thickness) mounted on a pole, which is connected to two force transducers for measuring forces in y- and z-direction. The levitation part is moveable in z-direction for positioning the YBCO bulk above the magnetic track to measure the levitation force at different gaps between the excitation part and the levitation part. The superconducting phase at $T_C = 92$ °K were activated by cooling the YBCO bulk with liquid nitrogen (LN_2) down to a temperature of 77 °K.

At first the YBCO bulk has been placed in a certain cooling height (CH) above the pm-arrangement (PM), shown in fig.1.

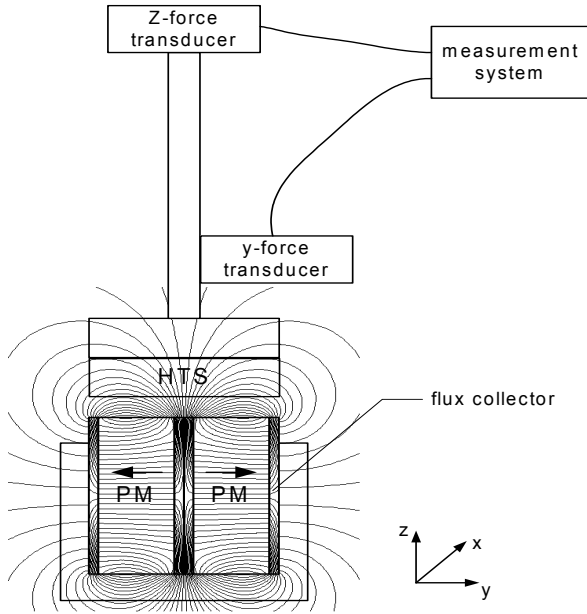


Fig. 1: System for measuring static force and stiffness

The High Temperature Superconductor (HTS) was then cooled down with LN_2 , until the HTS is completely in the superconducting state a series of vertical movements $\Delta z_{\text{HTS}} = \pm 0.5 \text{ mm}$ with an increment of 0.1 mm have been accomplished by moving the HTS-part.

For lateral force measurements the YBCO bulk has been placed centred above the excitation. After the HTS is completely below its critical temperature at $T_C = 92 \text{ °K}$ series of lateral movements $\Delta y_{\text{HTS}} = \pm 0.5 \text{ mm}$ with a increment of 0.1 mm has been accomplished by moving the excitation-part in y-direction. The approach to calculate the stiffness is described in chapter 3.2.

2.2 Damping measurement

For dynamic measurements a separate setup has been used. Here the excitation-part includes the PMs and is mounted on a table. The levitation-part is positioned above the excitation-part. A ferromagnetic plate is mounted on the top of the levitation-part as armature disc for the electromagnet, which is placed on top of the armature disc, mounted on a static frame. This apparatus, shown in fig. 2, is designed to investigate the damping characteristics of the SMB. After the HTS in the levitation-part is cooled below its critical temperature within the magnetic field of the excitation-part the distance-plate has been removed. The levitation-part is now levitating with an air gap due to the distance plate. To initialize the measurement the electromagnet will be activated to displace the levitation-part with Δz_0 . After the electromagnet is switched off the repositioning of the levitation-part starts and can be measured by a piezoelectric acceleration transducers mounted on the levitation-part.

To evaluate the measuring signal a measurement system with time base and FFT analyser has been used. The mechanical oscillation of the levitation-part during the repositioning process due to the interaction between magnetic field and the HTS illustrate the intensity of the magnetic flux pinning force.

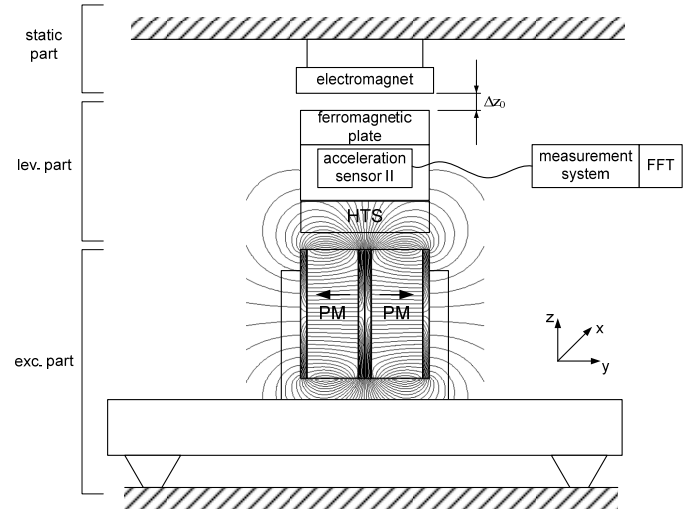


Fig. 2: Device for measuring damping

3 MEASUREMENT RESULTS

3.1 Force

Vertical force measurements have performed as a function of the cooling height and working height (WH), which depends on the weight of the levitation-part. In principle the quality of the vertical force between a HTS and a pm-arrangement has been investigated by zero-field-cooling and afterwards measuring the vertical force by reducing the gap between the HTS and the pm-arrangement. One can observe a repulsive force between HTS and PM cause of Meissner effect up to the lower critical magnetic field H_{C1} of the HTS. To design a stable linear SMB the behaviour of vertical and lateral forces due to a vertical or lateral displacement is very important. To improve the application in this point of view, which means to use the flux pinning effect in HTS the field-cooling-process is essential. The results of preliminary investigations for the chosen bearing configuration yielded a maximum CH of 8 mm for a sufficient vertical force (i.e. z-direction) by coexistent of a wanted lateral force (i.e. y-direction). In fig. 3 and fig. 4, the vertical force versus the vertical displacement and lateral force versus the lateral displacement of the HTS around the cooling position is shown as function of different CHs.

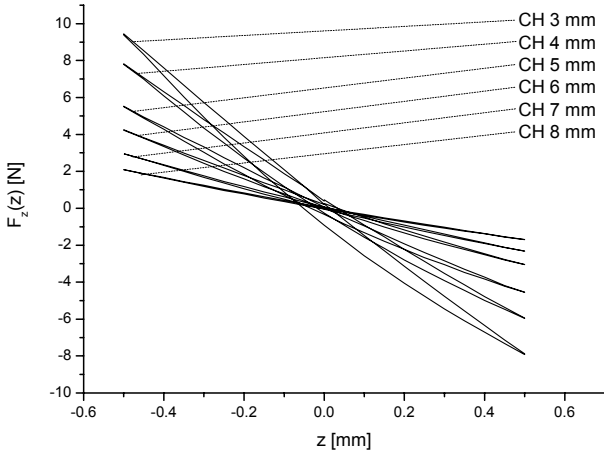


Fig. 3: Vertical force vs. vertical displacement

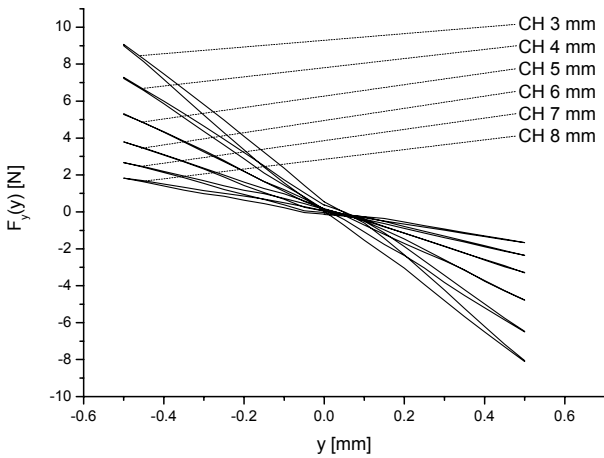


Fig. 4: Lateral force vs. lateral displacement

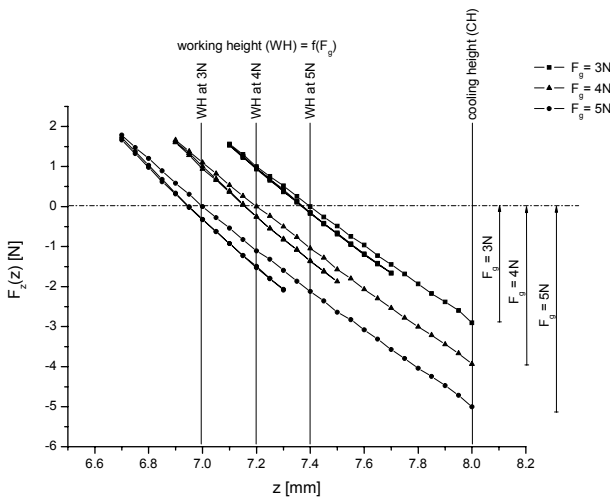


Fig. 5: Vertical transition-run CH to working point/ - line

After the HTS is in the superconducting state and the distance plate has been removed, a new working point (WP) will be adjusted due to the weight of the levitation-part. According to the curve for CH = 8 mm in fig. 3 it is possible to calculate the offset between CH and height of working point for different weights of the levitation-part. The measurement run

starts at CH with a negative offset due to the assumed weight. The gap has been reduced to the working point (force equilibrium) after this a loop ($\Delta z_{HTS} = \pm 0.3$ mm) around the working point has been started, shown in fig. 5.

The measuring forces due to the displacements along the new curve characterise the SMB with the given parameters in weight of levitation-part, CH and the maximum displacement depends of the technical requirements.

3.2 Stiffness

The stiffness has been calculated by evaluation the force measurements. Fig. 6 shows the vertical forces versus the vertical displacements, additional a polynomial fitting curve. The characteristic polynomial to fit the curve in fig. 6 is described as

$$y = A + B \cdot x + C \cdot x^2 .$$

The constants for the shown example in fig. 6 are:

$$A = 0; B = -17.3 \text{ and } C = 4.2.$$

In this case it is required to choose the parabolic polynomial or a polynomial with higher order to fit the curve in fig. 6. The derivative of the fit is the stiffness-function of the SMB.

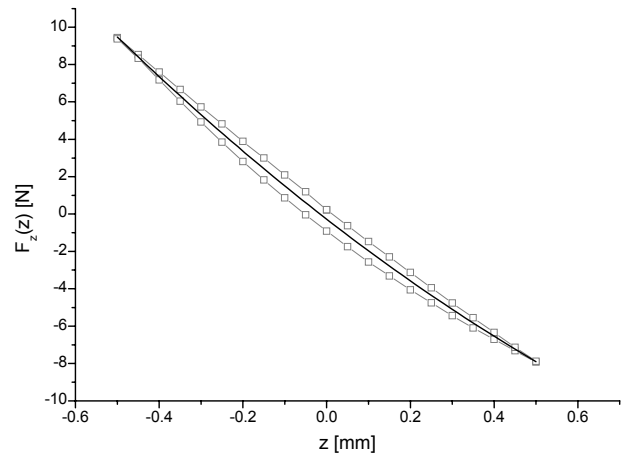


Fig. 6: Principle curve fitting to calculate the stiffness (i.e. loop measurement $\Delta z_{HTS} = \pm 0.5$ mm at CH = 3mm, WP = 3 mm)

The parabolic polynomial has been derivated and can be described as

$$\dot{y} = B + 2C \cdot x \rightarrow \dot{F}_z = -17.3 + 8.4 \cdot z .$$

The stiffness of the SMB is in this case a linear function, which depends on the CH and the maximum displacement Δz_{HTS} . As shown in fig. 7, the characteristic curves have a significant slope. Therefore a constant for the stiffness is suitable only in first approximation. To describe the mechanical dy-

namics more correctly a stiffness-function is required.

The stiffness-functions of the curves for the vertical force vs. vertical displacements, shown in fig. 7, give information about the quality of the SMB design (i.e. quality of the pm-arrangement and the quality of the superconductor material) to estimate the performance of the SMB in vertical direction. The same procedure is to repeat for lateral performance.

To characterise the SMB-behaviour at the working point further measurements get important. The stiffness-characteristics around the working point by a displacement $\Delta z_{HTS} = \pm 0.3$ mm has been calculated by fitting the force measuring curves shown in fig. 8. The parameters of the fitting curves for the three working points are shown in tab. 1.

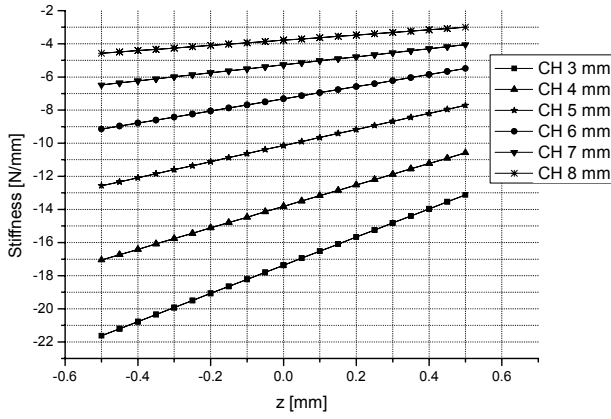


Fig. 7: Vertical stiffness vs. vertical displacement

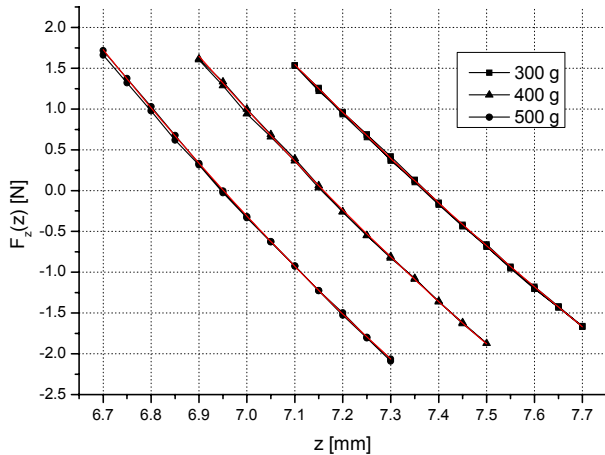


Fig. 8: Curve fitting to calculate the stiffness at three work points due to the weight of the levitation-part

Tab. 1: Parameters of fitting curves in different working points

working point	weight	A	B	C
1	300g	91	-19	1
2	400g	112	-25	1.3
3	500g	122	-28	1.6

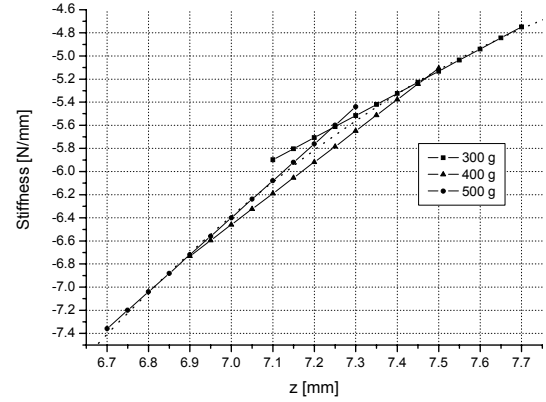


Fig. 9: Stiffness vs. displacement and the weight of the levitation-part

The stiffness functions, calculated similar to the example above, shown in fig. 9. The measuring curves for stiffness due to the weight and the working point are linear functions like tangents on a parabolic polynomial for the stiffness in the interval from $6 \leq z_{HTS} \leq 8$. This parabolic stiffness polynomial is shown as a dotted line in fig. 9 and can be described as

$$\text{Stiffness} = -1.08 \cdot z_{HTS}^2 + 18.3z_{HTS} - 81.2,$$

for the interval: $6\text{mm} \leq z_{HTS} \leq 8\text{mm}$.

The significant influence of the vertical displacement on the vertical stiffness of the SMB additional the dependence of the weight of the levitation part as shown in fig. 8 and fig. 9 is an important fact. In first approximation the transfer-behaviour can be simulated with a constant value for the vertical stiffness of a SMB. For an exact simulation model a parabolic polynomial function has assumed to describe the stiffness in a specific work interval.

3.3 Damping

The damping measurements have been accomplished to investigate the third constant (attenuation constant d) to describe the transfer behaviour in vertical direction using the equation of motion. The measuring system, shown in fig. 2, is designed to investigate the system with variable mechanical excitations. To investigate the attenuation constant due to the vertical displacement and the weight an additional force in vertical direction coming from an electromagnet has been generated an initial value for the displacement (i.e. $\Delta z_0 = +0.3$ mm). To start the

measurement the electromagnet will be deactivated and the mechanical oscillation of the levitation part starts. The run of the acceleration of the levitation-part vs. the time is shown in fig. 10. The attenuation constant can be analyzed by covering the damped oscillation curve by an exponential function, the envelope.

The characteristic equation for this envelope is described as

$$x = \overset{\square}{x_0} e^{-\delta t},$$

where δ is the decay constant. The envelope has been fitted by the coordinates of the local maximum of the damped oscillation. The fitted and standardised curve a^* can be described as

$$a^* = 1 \cdot e^{-3.2174 \cdot t}.$$

The attenuation constant is described as

$$d = 2 \cdot m \cdot \delta = 1.0488 \frac{kg}{s}$$

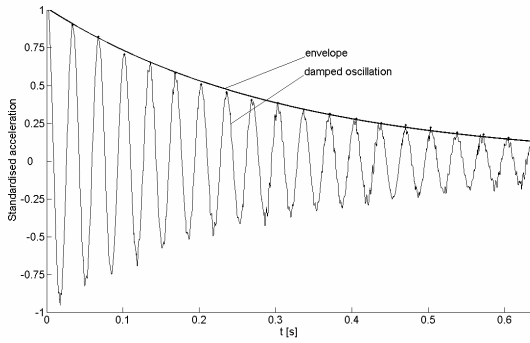


Fig. 10: Damped mechanical oscillation and envelope of the levitation-part

4 DISCUSSION

The allowed load of the levitation-part in the first experimental setup was $m_{\max} = 170$ g. The curve in fig. 10 shows the acceleration of a levitation-part (i.e. $m_{ip} = 163$ g) vs. the time and the envelope of the damped oscillation curve. The superconducting magnetic bearing is modulated by a harmonic oscillation model with mechanical constants, shown in fig. 11.

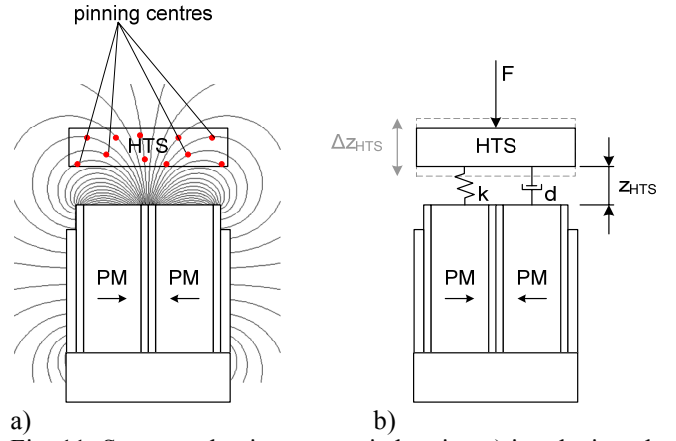


Fig. 11: Superconducting magnetic bearing a) is substitute by a mechanical oscillation model b)

All dynamic characteristics of the superconducting magnetic bearing can be calculated by the decay constant δ and the mass m . The equation of motion for the mechanical model can be described as

$$m\ddot{z} + d\dot{z} + kz = 0.$$

The characteristic constants mass m , attenuation constant d and stiffness k are the specific constant/functions for the introduced model. In the first approximation only constants for m , d and k , no functions, have been used. The calculation of this characteristic constants and further interesting system parameters for the damped oscillation are

$$\text{Damped oscillation} \quad z(t) = \hat{z} \cdot e^{-\delta \cdot t} \cdot \sin(\omega_d t + \varphi_0)$$

System parameters

$$\text{Decay constant} \quad \delta = 3.2174 \cdot s^{-1}$$

Characteristic angular frequency of the damped oscillation

$$\omega_d = \frac{2\pi}{T_d} = \frac{2\pi}{0.033569} = 187.2 \text{ Hz}$$

Eigen angular frequency

$$\omega_0 = \sqrt{\omega_d^2 + \delta^2} = 187.0 \text{ Hz}$$

Damping ratio

$$D = \frac{\delta}{\omega_0} = 0.0172$$

Constants of equation of motion

$$\text{Mass} \quad m = 0.163 \text{ kg}$$

$$\text{Attenuation constant} \quad d = 2 \cdot m \cdot \delta = 1.0488 \frac{kg}{s}$$

Stiffness constant $k = \omega_0^2 \cdot m = 5.7 \frac{N}{mm}$

The calculated stiffness constant of the damped oscillation confirms the measured value, shown in fig. 9. To compare the interaction between the applied magnetic field and the superconducting bulk with the mechanical oscillator is an appropriate approach to characterise a superconducting magnetic bearing.

5 SUMMARY

Conclusions obtained in this research are summarized as follows:

- 1) The weight of the levitation part determines the working point of a SMB. Since the overall behaviour such as vertical and lateral stiffness is strongly influenced by the working point, the levitation weight is a crucial parameter for designing the SMB.
- 2) The verification of the measurement results from the setup for static force and stiffness measurements with the results from the dynamic experimental setup has been accomplished successfully.
- 3) To describe the SMB by a harmonic oscillator by means of mechanical parameters to investigate the dynamic behaviour was proposed and applied to simulate the dynamic behaviour.

REFERENCES

- Beyer, C., de Haas, O., Verges, P. & Schultz, L. 2004: Design of the guideway for the SupraTrans project: *Proceedings Maglev 2004, Shanghai, China*: 333-338
- de Haas O., Schultz L., Verges P., Beyer C., Röhlig S., Olsen H., Kühn L., Berger D., Noteboom U. 2004. Superconductively levitated transport system – the SupraTrans project: *Proceedings Maglev 2004, Shanghai, China*: 326-332
- Futamura M., Maeda T., Konishi H. 1998: Damping Characteristics of a Magnet Oscillating above a YBCO Superconductor: *Jpn. J. Appl. Phys.* 37: 3961-3964
- Hull J.R. and Cansiz A. 1999. Vertical and lateral forces between a permanent magnet and a high-temperature superconductor: *J. Appl. Phys.* 86(11): 6396-6404
- Sugiura T., Tashiro M., Uematsu Y. and Yoshizawa M. 1997: Mechanical Stability of a High- T_c Superconducting Levitation System: *IEEE Trans. Appl. Supercond.* 7(2), 386-389
- Weinberger B.R., Lynds L. and Hull J.R. 1990: Magnetic bearings using high-temperature superconductors: some practical considerations: *Supercond. Sci. Technol.* 3: 381-388